ELSEVIER

Nuclear Physics B (Proc. Suppl.) 113 (2002) 277–281

NUCLEAR PHYSICS B
PROCEEDINGS
SUPPLEMENTS

www.elsevier.com/locate/npe

MICROSCOPE MISSION AND PERFORMANCE

R. Chhun[a], M. Rodrigues[a] and P. Touboul[a]

[a]Physics and Instrumentation Department
ONERA, Office National d'Études et de Recherches Aérospatiales
BP 72, 92322 Châtillon Cedex, France

Scheduled for a launch in 2005, the MICROSCOPE mission aims at testing the universality of free-fall, one of the most known manifestations of the equivalence principle (EP). To increase by a few orders of magnitude the experimental accuracy of the EP test up to an accuracy of 10^{-15}, the MICROSCOPE mission will mainly take advantage of the calm in-orbit environment and the very long free-fall duration for the integration of the measurement. The instrument is composed of two differential electrostatic accelerometers, each of which is composed of two cylindrical and concentric test-masses. The masses of one accelerometer will both be made of the same material, Platinum, in order to demonstrate the accuracy of the experiment. In the second one, one mass will be made of Platinum, the other of Titanium. The EP test will be performed by measuring the force necessary to equalize the rate of fall of these two materials. This document presents the concept and design, presently developed at ONERA, of such a space payload. The most critical elements of the instruments are detailed to point out what mainly sets the test accuracy. Last experimental investigations concerning the main performance limitation are also mentioned.

1. Historical and present context

Over the previous two decades much effort has been paid in physics laboratories on the development of experiments dealing with the test of Equivalence Principle (EP) or on the search for new interactions or a new gravitational potential. Improvement in the confirmation of the equivalence between inertial mass and gravitational mass represents an important verification of the relativistic theory of gravitation and of other metric theories which postulate this principle. The current structure of modern physics is composed of the two theories of "quantum mechanism" and "general relativity". The separation lies on the fact that general relativity is a purely classical (non quantic) theory. Ambitious unification theories (super strings theory, great unification theory...) aiming to merge general relativity and quantum physics, predict the existence of a new interaction which could act at macroscopic scales. Whatever the origins of such a new force could be, one of its consequences, when added to the gravitation, should be an observable violation of the Equivalence Principle at levels lower than 10^{-14} [1]. More accurate tests of the Equivalence Principle are then very useful to define the parameters of those unification theories. Ground based experiments [2,3] are limited by the duration of free fall and by the acceleration noises (seismic and anthropic). To be able to reach an accuracy better than 10^{-14}, the future tests will have to be performed in space. A Galileo-like experiment in orbit will take advantage of a quiet acceleration environment and of a quasi-unlimited free fall duration. In such a frame an international cooperation NASA/ESA has devoted the STEP mission to test the Equivalence Principle with a precision of 10^{-18}. Considering that such a level of accuracy will raise many technical problems, the MICROSCOPE (*MICROSatellite pour l'Observation du Principe d'Équivalence*) space project is proposed as a stage to the necessary progress. The accuracy goal of MICROSCOPE is 10^{-15} which is quite three orders of magnitude more accurate than the present state of the art.

2. The Microscope mission scenario

The MICROSCOPE mission has been selected within the CNES microsatellite science program. The satellite is to be launched in 2005 on board a DNEPR launcher, its weight will not exceed 150 kg and its payload power will be less than 40 W. The circular and sun-synchronous orbit will enable reduced tem-

PII S0920-5632(02)01852-2

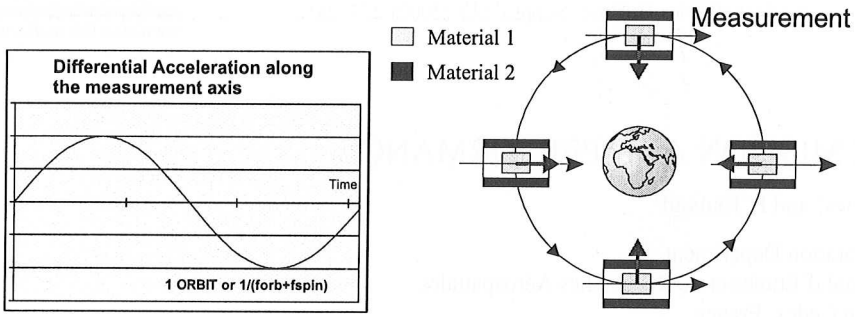

Figure 1. Principle of a differential acceleration measurement between two controlled concentric test-masses. Black arrow: the instrument axis, red arrow: the Earth (source) gravity field of the EP test.

perature variations due to eclipse [4]. The orbit eccentricity is limited to less than 10^{-2} for an altitude of 700 km. The satellite will carry two electrostatic differential accelerometers compatible with a room temperature experiment. One of them will be a zero experiment to test the accuracy of the measurement while the other will test the EP. To the benefit of the experiment accuracy, electrical thrusters will assure a continuous drag compensation. Continuous drag-free technology has never been performed but is required for future fundamental physics missions (STEP, LISA, GOCE,...).

The different phases of the EP test mission, the orbit acquisition, the operation and the verification of the instruments and of the drag-free system, the calibration and the verification of the experiment will spread over a total duration of one year. The resolution of each accelerometer in order to be compatible with the 10^{-15} accuracy and the 10^5 s integration time of the measured signal is $10^{-12}\,\mathrm{m\,s^{-2}}/\sqrt{\mathrm{Hz}}$ at the EP test frequency f_{EP} very near to 10^{-3} Hz.

Unlike Galileo-type experiments based on the measurement of differences between two test-masses trajectory submitted to the same gravity field, in the MICROSCOPE experiment the two test-masses of one differential accelerometer will be maintained motionless with respect to each other, the measurement being the acceleration needed to compensate a hypothetical violation of the universality of free fall law. The signal to be detected (if any) will be at a well known phase and frequency, the orbital frequency modulo the rotation frequency of the satellite about the axis normal to the orbital plane (see fig. 1).

3. Single accelerometer concept

Servo-controlled electrostatic accelerometer is based on the measurement of the electrostatic force necessary to maintain the accelerometer test-mass motionless with respect to the sensor cage surrounding it [5]. For space applications the test-mass is fully suspended on its six degrees of freedom, suppressing all mechanical contact to the benefit of the resolution. The performance relies on the resolution of the test-mass position sensor [6], on the very limited stiffness of the test-mass with respect to the accelerometer cage and on the weak level of the test-mass motion disturbances Γ_{env} due to the environment.

As depicted in fig. 2, the test-mass is kept motionless in position and attitude by means of six servo-controlled channels acting independently. The pairs (one, two or four depending on which degree of freedom) of electrodes corresponding to each loop is used for both capacitive position sensing and electrostatic force actuation. From the measurement of the capacitive sensor a digital corrector determines what voltages to apply back on the electrodes. These voltages generates electrostatic fields and pressures on the mass to maintain its position at the center of the electrode cage. Through a thin gold wire ($\varnothing = 5\,\mu$m, $1.5\,\mathrm{cm} < L < 2\,\mathrm{cm}$) a continuous and a sine wave voltages are applied to the test-mass. The first one, V_p,

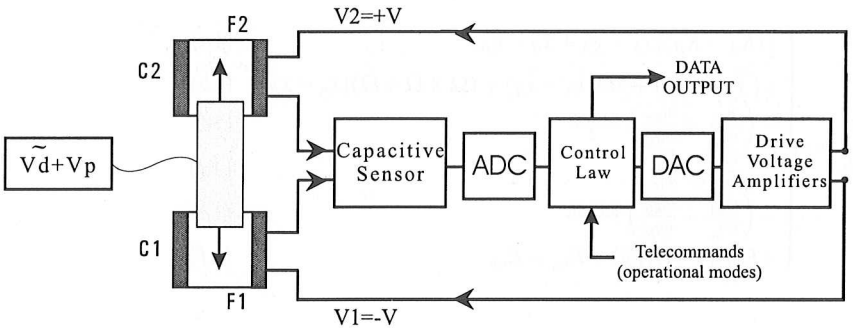

Figure 2. Accelerometer control loop scheme for one axis

is used to linearize the electrostatic restoring forces. The second one, V_d, is needed for the capacitive sensing of the test-mass motion.

One of the advantages of the electrostatic suspension is the generation of weak forces with a measurable level of corresponding voltage. With the position of the test-mass being servo-controlled, the relative motion of the test-mass with respect to the cage can be maintained almost null in the frequency bandwidth of the suspension in which the gain of the servo-loop is important. Optimizing the accelerometer thus aims at reducing the noise of the loop electronics, the stability of the mass/instrument configuration, the disturbances of the mass motion in order to provide a well identified acceleration represented by the electrostatic suspension forces.

4. Differential accelerometer concept

From the signals recorded by two accelerometers, the difference of measurement between them can be split leading to eq. 1 with x_i the mass$_i$ position with respect to the inertial frame. Expression (1e) is the signal to be detected in case of an EP violation. The other terms are maintained weak during the space experiment. In term (1a) the difference of the common acceleration is weak because of the drag compensation (less than $3 \times 10^{-10}\,\mathrm{m\,s^{-2}}/\sqrt{\mathrm{Hz}}$) and also noticeably reduced by the in-orbit matching of the accelerometer scale factors during calibration phase, the $(K_A - K_B)$ matrix components being less than 3×10^{-4}. In term (1b) the servo-control maintains the relative motion of the two test-masses by maintaining them motionless with respect to the same electrode cylinder support. The misplacement of the test-masses is already weak ($< 20\,\mu$m) and can be restored from the measurement to an almost null value ($< 0.1\,\mu$m). The attitude control of the satellite limits the angular velocity Ω to less than $10^{-6}\,\mathrm{rd\,s^{-1}}/\sqrt{\mathrm{Hz}}$ and the acceleration $\dot{\Omega}$ to less than $10^{-8}\,\mathrm{rd\,s^{-2}}/\sqrt{\mathrm{Hz}}$. In term (1c) the concentricity of the test-masses limit the gravity gradient effect. The shape and dimensions of the test-masses are then selected to limit the effect of the self gravity gradient of the satellite, which may fluctuate with temperature [7]. Term (1d) represents the non gravitational parasitic accelerations (radiation pressure, radiometer effect). Eventually in term (1f) are gathered the instrument noise including non linearity and measurement electronics noise.

5. Instrument description

The materials of the test-masses have been selected according to their theoretical atomic properties [8] and also considering homogeneity, machining possibility, thermal stability, magnetic properties, density, electrical conductivity... This criteria have led to the choice of Platinum and Titanium. Alternative material to Titanium, such as Copper alloys are under study; such materials could offer higher density (better EP test performance) and have similar atomic number to Titanium. The dimensions of the test-masses are selected in order to limit disturbing gravity effect of moving masses located around the

$$\frac{\hat{F}_A}{m_{I_A}} - \frac{\hat{F}_B}{m_{I_B}} \approx \begin{cases} \frac{1}{2}(K_A - K_B)(\ddot{x}_A - g_A + \ddot{x}_B - g_B) & (1a) \\ +(\overset{\circ\circ}{x}_A - \overset{\circ\circ}{x}_B) + 2\Omega(\overset{\circ}{x}_A - \overset{\circ}{x}_B) + (\Omega \times \Omega + \overset{\circ}{\Omega})(x_A - x_B) & (1b) \\ -\left(\frac{m_{g_A}}{m_{I_A}} + \frac{m_{g_B}}{m_{I_B}}\right)\frac{g_A - g_B}{2} & (1c) \\ -\left(\frac{F_{P_A}}{m_{I_A}} - \frac{F_{P_B}}{m_{I_B}}\right) & (1d) \\ -\left(\frac{m_{g_A}}{m_{I_A}} - \frac{m_{g_B}}{m_{I_B}}\right)\frac{g_A + g_B}{2} & (1e) \\ +E(F_A) - E(F_B) + E_{n_A} - E_{n_B} & (1f) \end{cases} \quad (1)$$

instrument. A mass M at distance R from the two test-masses creates not only a common acceleration, a, but also a differential one, Δa, which can be confused with an EP violation signal. In order to minimize $\Delta a/a$, the radiuses and length of the cylinders must be chosen accurately leading to an equality of the moments of inertia around every axis for each test-mass (see fig. 3). The cages of the accelerometers are made of silica, the electrodes for the electrostatic suspension defined on the cylinder cages are gold-coated. The axial control (X axis) consists in two ring electrodes covering the exterior ends of the test-masses. The radial control (Y,Z axes) consists in 4 electrodes for each axis, located on the inner cylinder and controlling both translation and rotation. The spin control (around X axis) consists in 4 pairs of electrodes facing each a plane surface located on the exterior surface of each test-mass.

As the flight models can not be tested under g because of the heavy weight of each test-mass, specific silica test-masses should be mounted instead of heavy masses to allow ground tests on the engineering models. Flight models should be tested before launch in ZARM free fall tower whose members are presently working to improve their free-flyer drop capsule performances in the order of a few tens of nano-g compatible with the operation range of the MICROSCOPE instrument. Unlike previous space missions (CHAMP [9], GRACE [10]) the control electronics is to be digital for an easy change of the control laws and an adapted calibration process [11].

6. Performance

The accelerometer performances are limited by several noises, most important of which is due to the gold wire particularly needed to maintain the neutrality of the test-mass electrical charge when crossing particle fluxes or at the switch-on at the first test-mass levitation. Other systems, such as UV flashing, are possible but need a more complex interface. In spite of the 5 μm diameter, this gold wire remains an unavoidable mechanical link between the test-mass and the cage which means an additional parasitic stiffness and damping. The gold wire stiffness k_{wire} coupled with the position noise generates an acceleration noise:

$$\Gamma_{n,k} = \frac{k_{wire}}{m} x_n. \quad (2)$$

The gold wire damping H_{wire} generates a thermodynamic acceleration noise (Nyquist theorem):

$$\Gamma_{n,H} = \frac{1}{m}\sqrt{4k_B T H_{wire}}. \quad (3)$$

This noise is currently estimated, from our recent H_{wire} measurements, at about $10^{-12}\sqrt{\frac{10^{-3}\text{Hz}}{f}}\,\text{m s}^{-2}/\sqrt{\text{Hz}}$. This noise contribution dominates all other electronic noises, bias fluctuation, thermal sensitivity... A particular effort is paid to identify the two critical values that are the stiffness and the damping of the gold wire. A simple model of the gold wire stiffness being in $radius^4/length^3$ gives the drivers to limit the parasitic effects of the wire: the gold wire should be chosen as thin as possible and as long as possible. Considering availability and machining constraints, the dimensions selected are the ones mentioned before ($\varnothing = 5\,\mu$m, $1.5\,\text{cm} < L < 2\,\text{cm}$). Tests are underwent at present time with a dedicated instrument developed in ONERA [12] to confirm the last measured gold wire damping and stiffness compatible with the MICROSCOPE requirements.

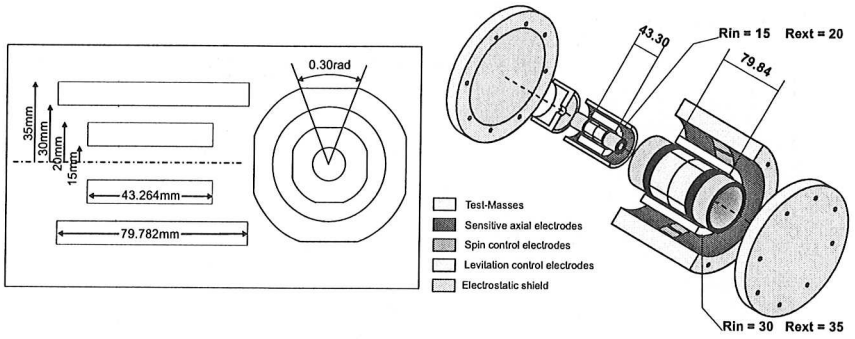

Figure 3. Configuration and dimensions of the test-masses in one MICROSCOPE differential accelerometer

7. Conclusion

A few ground experiments dedicated to assess some of the MICROSCOPE performance limiting items have been conducted and enable to envisage to test the EP with 10^{-15} accuracy and an improvement by a thousand with respect to laboratory tests. A prototype with a Silica test-mass has been developed in order to levitate the test-mass under one g. This prototype has already been integrated and showed the feasibility of the experiment mechanical design as well as the needs for specific integration and verification procedures such as the centering of the test-masses [13]. The on-ground tests also require free-fall testing, specifically in the drop tower of the ZARM laboratory of the University of Bremen. The four seconds of drop under nanogravity has to be assessed with the optimization of the existing free-flyer.

8. Acknowledgment

The analysis of the Equivalence Principle test in space and the development of the MICROSCOPE accelerometers are carried out at ONERA under a CNES contract and with the cooperation of CERGA/OCA and the ZARM institute in Bremen University.

REFERENCES

1. Fayet P., proceedings COSPAR 33, Warsaw, 2000.
2. Braguinsky VB. & Panov VL., Verification of inertial and gravitational mass, *in* Soviet Physics, **34**, pp 463-466, 1972.
3. Adelberger EG., Stubbs BR., Heckel BR., Su Y., Swanson HE. & al., *in* Physical Review D, **42**, 3267, 1990.
4. Bernard A., Gay M. & Juillerat R., The Accelerometer CACTUS, *in* AGARDograph, **254**, 1982.
5. Touboul P., Foulon B. & al., Electrostatic space accelerometers for present and future missions, Acta Astronautica, **45**, 10, pp 605–617, 1999.
6. Josselin V., Capacitive detection scheme for space accelerometers, *in* Sensors & Actuators A: Physical, 1999.
7. Connes A., Damour T. & Fayet P., Aspherical gravitational monopoles, *in* Nuclear Physics, 1996.
8. Damour T. & Blaser JP., Optimizing the choice of the materials *in* EP experiments, XXXèmes rencontres de Moriond, 1995.
9. Champ mission, http://op.gfz-potsdam.de/champ/
10. Grace mission, http://op.gfz-potsdam.de/grace/
11. Josselin V., Digital electronics for electrostatic accelerometers: interest for high resolution and in-orbit calibration, *in* Bolettino di Geofisica Teorica ed Applicata, 1998.
12. Willemenot E., Thesis, Pendule de torsion à suspension électrostatique, très hautes résolutions des accéléromètres spatiaux pour la physique fondamentale, ONERA, June 1997.
13. Lafargue L., Thesis, Configuration mécanique d'accéléromètres électrostatique pour le test en orbite du Principe d'Équivalence, ONERA, June 1997.